

Double-giant-dipole resonance in ^{208}Pb

S. Nishizaki

Faculty of Humanities and Social Sciences, Iwate University, 3-18-34 Ueda, Morioka 020, Japan

J. Wambach

Institut für Kernphysik, Technische Universität Darmstadt, Schloßgartenstraße 9, D-64289 Darmstadt, Germany

(Received 23 October 1997)

Double-dipole excitations in ^{208}Pb are analyzed within a microscopic model explicitly treating $2p2h$ excitations. Collective states built from such excitations are shown to appear at about twice the energy of the isovector giant dipole resonance, in agreement with experimental findings. The calculated cross section for Coulomb excitation at relativistic energies cannot explain simultaneously the measured single-dipole and double-dipole cross sections, however. [S0556-2813(98)01003-6]

PACS number(s): 21.60.-n, 24.30.Cz, 25.70.De

Double-giant-dipole resonances (DGDR) have been observed in pion double-charge-exchange reactions at LAMPF [1] as well as with relativistic heavy ions at GSI [2]. In peripheral heavy-ion collisions the excitation proceeds via the Coulomb interaction. At relativistic energies there is a strong focusing of the electromagnetic field in the target rest frame. This greatly enhances the intensity in the vicinity of the target nucleus, thus increasing the probability for two-photon absorption from the ground state.

The global parameters of the DGDR, i.e., the resonance energy E_{DGDR} , the width Γ_{DGDR} , and the cross section σ can be summarized as follows [3].

(1) The resonance energy is about twice that of the isovector giant dipole resonance (GDR) $E_{\text{DGDR}} \approx 2E_{\text{GDR}}$ suggesting an interpretation as an independent two-phonon state.

(2) The observed values of the width Γ_{DGDR} are bracketed by $\sqrt{2}\Gamma_{\text{GDR}}$ and $2\Gamma_{\text{GDR}}$, again supporting a harmonic picture.

(3) The measured Coulomb cross section σ_{exp} is larger than the theoretical estimate σ_{th} . The values for the ratio $\sigma_{\text{exp}}/\sigma_{\text{th}}$ are scattered between 1 and 5 depending on the nuclei considered and on the theoretical analyses. This puts some doubt on the interpretation of the DGDR as an independent two-phonon state.

To reach a quantitative understanding of the DGDR characteristics we carry out microscopic calculations for the DGDR in ^{208}Pb . The structure of the double-dipole states is investigated by diagonalizing the model Hamiltonian in the space of $1p1h$ and $2p2h$ excitations. For comparison with experiment the cross section for Coulomb excitation—based on the second-order perturbation theory—is calculated.

The nuclear structure model has been developed in our previous work [4] on double-dipole excitations in ^{40}Ca . We give a brief summary, stressing some new aspects in the application to heavy nuclei such as ^{208}Pb . The eigenstates $|n\rangle$ of the nuclear Hamiltonian \hat{H}_0 are determined by diagonalization in the space of $1p1h$ and $2p2h$ excitations. As a model space of single-particle states, we take into account three major shells of the Woods-Saxon potential on both sides of the Fermi level. The continuum states are discretized via expansion in a harmonic oscillator basis. The number of $2p2h$ states resulting from the single-particle basis exceeds several hundred thousand. Most of them, however, have van-

ishingly small matrix elements for the double-dipole transition. Thus we select only those $2p2h$ states whose excitation energies are below 40 MeV and whose double-dipole matrix element exceeds a lower limit, specified by

$$|\langle 2p2h | \hat{D} \hat{D} | 0 \rangle|^2 / \sum_2 |\langle 2 | \hat{D} \hat{D} | 0 \rangle|^2 \geq 5 \times 10^{-5}. \quad (1)$$

Here, the isovector dipole operator \hat{D} is defined as

$$\hat{D} = e \frac{N}{A} \sum_{i=1}^N \mathbf{r}_i - e \frac{Z}{A} \sum_{i=1}^N \mathbf{r}_i. \quad (2)$$

With these conditions, the number of $2p2h$ states can be reduced to 996 for the $J^\pi = 0^+$ double-dipole transition and to 2011 for the $J^\pi = 2^+$ transition. The amount of transition strength lost is less than a few percent.

The mean energy and total strength of the GDR in ^{208}Pb , calculated in the usual $1p1h$ RPA with the nuclear Hamiltonian [4] including a density-dependent zero-range interaction, are 10.8 MeV and 96% of the TRK sum-rule value, respectively. Both are smaller than the photoneutron data [5] which yield 13.4 MeV and 134%. Therefore we enhance the theoretical results by a scaling of the single-particle energies according to $\varepsilon_{\text{sp}} = \varepsilon_{\text{WS}} / (m^*/m)$ with the effective mass $m^*/m = 0.75$. By this procedure, we obtain the mean energy and the total strength as 13.5 MeV and 126% of the TRK value, in good agreement with experiment.

The strength distributions of the double-dipole transition are shown in Fig. 1. Figures 1(a) and 1(b) [1(c) and 1(d)] represent the unperturbed and the perturbed strength distributions for the 0^+ (2^+) double-dipole transitions, respectively. Both for 0^+ and 2^+ double-dipole transitions, the perturbed strength concentrates in the region of 25–30 MeV. There appear several states which carry about ten times more strength than the strongest unperturbed ones. The mean energy $\langle E \rangle$ and the width Γ are estimated in terms of the energy moments

$$m_{DD}^k = \int dE E^k S_{DD}(E),$$

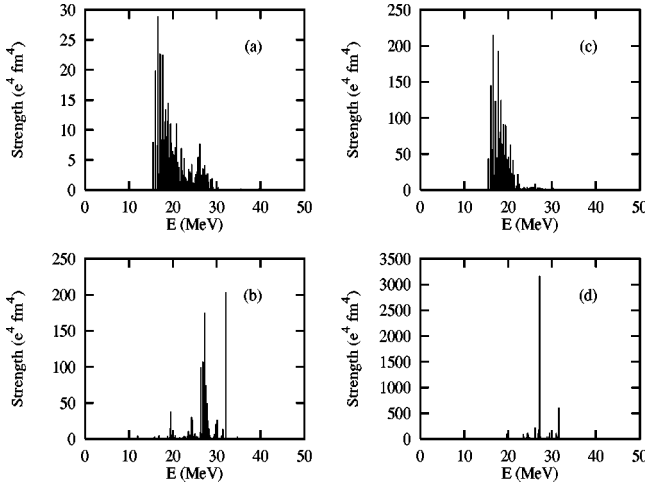


FIG. 1. Double-dipole strength distributions in ^{208}Pb . (a) Unperturbed 0^+ DD strength. (b) Perturbed 0^+ DD strength. (c) Unperturbed 2^+ DD strength. (d) Perturbed 2^+ DD strength.

$$S_{DD} = \sum_n |\langle n | \hat{D}\hat{D} | 0 \rangle|^2 \delta(E - E_n), \quad (3)$$

as

$$\langle E \rangle_{\text{DGDR}} = m_{DD}^1 / m_{DD}^0 \quad (4)$$

and

$$\Gamma_{\text{DGDR}} = \sqrt{m_{DD}^2 m_{DD}^0 - (m_{DD}^1)^2} / m_{DD}^0, \quad (5)$$

and similarly for the isovector dipole excitations. The $\langle E \rangle_{\text{DGDR}}$ and Γ_{DGDR} are found to be 26.66 MeV (26.23 MeV) and 3.39 MeV (3.24 MeV) for 0^+ DGDR (2^+ DGDR), respectively. The mean energy of the DGDR is about twice that of the GDR. The calculated width, which corresponds to the fragmentation width (Landau damping) is larger than that of the GDR ($\Gamma_{\text{GDR}} = 2.90$ MeV) by the factor of 1.12–1.17. We note that the observed width includes, in addition, the escaping and spreading widths which are not treated in the present calculation.

In the semiclassical approach [6,7], the cross section for Coulomb excitation is given by

$$\sigma_{i \rightarrow f} = 2\pi \int_{R_{\min}}^{\infty} b db \frac{1}{2J_i + 1} \sum_{M_i, M_f} |a_{fi}|^2. \quad (6)$$

The projectile is assumed to move on a straight-line trajectory with impact parameter b . The minimum impact parameter R_{\min} is a key parameter, since the cross section sensitively depends on it as will be shown below.

The main components of the DGDR are $2p2h$ states, which are excited via a two-body operator of double-dipole

character ($\hat{D}\hat{D}$). For Coulomb excitation the precise form of the excitation operator is derived from the second order amplitude

$$a_{fi}^{(2)} = \frac{1}{(i\hbar)^2} \left\langle f \left| \int_{-\infty}^{+\infty} dt \int_{-\infty}^t dt' e^{+i\hat{H}_0 t / \hbar} \hat{V}(t) e^{-i\hat{H}_0 t / \hbar} \right. \right. \\ \left. \left. \times e^{+i\hat{H}_0 t' / \hbar} \hat{V}(t') e^{-i\hat{H}_0 t' / \hbar} \right| i \right\rangle, \quad (7)$$

where \hat{H}_0 and \hat{V} are the nuclear Hamiltonian and the Coulomb interaction between the projectile and target nuclei, respectively. To obtain the two-body operator, we exchange the order of $\hat{V}(t)$ [$\hat{V}(t')$] and $\exp(+i\hat{H}_0 t / \hbar)$ [$\exp(-i\hat{H}_0 t / \hbar)$]. This yields a series expansion in the times t and t' which includes single and multiple commutators of \hat{H}_0 and \hat{V} . In the limit of a ‘‘fast collision’’ [8], one only needs to take into account the lowest order in time. Finally the expression for the second-order amplitude of the double $E\lambda'$ transition is given by

$$a_{fi}^{(2)} = \left(4\pi \frac{Ze}{i\hbar} \right)^2 \sum_{\mu} \frac{(-)^{\mu}}{(2\lambda' + 1)^2} \left\{ \frac{1}{2} \langle f | \mathcal{N}_{EE}^{\lambda\lambda'}(\lambda, -\mu) | i \rangle \right. \\ \times [T_{\lambda\mu}^{E\lambda'E\lambda'}(\omega, \omega) + \hbar\omega U_{\lambda\mu}^{E\lambda'E\lambda'}(\omega, \omega)] \\ + \langle f | \mathcal{K}_{EE}^{\lambda\lambda'}(\lambda, -\mu) | i \rangle \\ \left. \times \frac{i}{2\pi} \mathcal{P} \int_{-\infty}^{+\infty} \frac{dq}{q} U_{\lambda\mu}^{E\lambda'E\lambda'}(\omega - q, \omega + q) \right\}, \quad (8)$$

with

$$T_{\lambda\mu}^{\pi_1\lambda_1\pi_2\lambda_2}(\omega_1, \omega_2) = [S_{\pi_1\lambda_1}(\omega_1) \otimes S_{\pi_2\lambda_2}(\omega_2)]_{\lambda\mu}, \quad (9)$$

$$U_{\lambda\mu}^{\pi_1\lambda_1\pi_2\lambda_2}(\omega_1, \omega_2) = [S_{\pi_1\lambda_1}(\omega_1) \otimes R_{\pi_2\lambda_2}(\omega_2)]_{\lambda\mu}, \quad (10)$$

$$\mathcal{N}_{\pi_1\pi_2}^{\lambda_1\lambda_2}(\lambda, \mu) = [\mathcal{M}(\pi_1\lambda_1) \otimes \mathcal{M}(\pi_2\lambda_2)]_{\lambda\mu}, \quad (11)$$

$$\mathcal{K}_{\pi_1\pi_2}^{\lambda_1\lambda_2}(\lambda, \mu) = \{ [H_0, \mathcal{M}(\pi_1\lambda_1)] \otimes \mathcal{M}(\pi_2\lambda_2) - \mathcal{M}(\pi_1\lambda_1) \\ \otimes [H_0, \mathcal{M}(\pi_2\lambda_2)] \}_{\lambda\mu}. \quad (12)$$

Here, $\mathcal{M}(\pi\lambda)$ denotes electric ($\pi = E$) or magnetic ($\pi = M$) multipole operators, while $S_{\pi\lambda}$ and $R_{\pi\lambda}$ are orbital integrals [7,8]. The principal-value integral in Eq. (8) results from a step function, which appears when the upper limit of the integral in Eq. (7) is extended to infinity. In the present estimate for the cross sections, we neglect this principal value integral.

The calculated cross section for Coulomb excitation of the DGDR with a ^{208}Pb projectile incident on a Pb target at 640 MeV/A is plotted as the solid line in Fig. 2. The dashed and dotted lines display the cross sections for the GDR and the GQR (giant quadrupole resonance), respectively. For comparison the former has been multiplied by the factor of 0.1. To account for the experimental energy resolution, the calculated cross sections have been smoothed by using a Breit-Wigner function of width 1.5 MeV. The main peak of the DGDR appears in the region of 25–30 MeV, just above the broad isovector GQR which appears around 20 MeV. The peak energy of the DGDR is about twice that of the GDR.

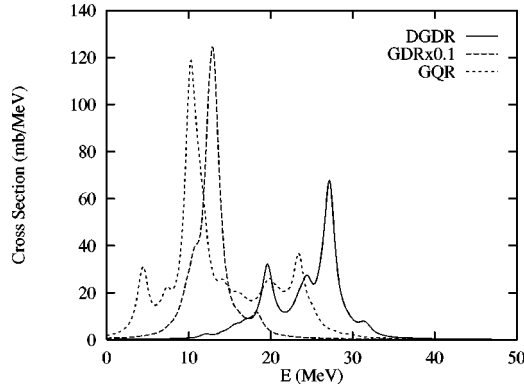


FIG. 2. Cross section for the Coulomb excitation in a Pb+Pb collision at 640 MeV/A. The solid line denotes the cross section of the DGDR while the dashed line displays the GDR cross section (multiplied by 0.1). In addition, the cross section for the GQR is shown as the dotted line. The minimum impact parameter is the value of case (b) (see text).

Next we discuss the dependence of the energy-integrated cross section on the minimum impact-parameter R_{\min} which is parametrized as $R_{\min} = r_0(A_t^{1/3} + A_p^{1/3})$, where A_t and A_p denote the mass number of target and projectile nuclei, respectively. Three cases are considered: (a) $r_0 = 1.50$ fm, (b) $r_0 = 1.31$ fm, and (c) $r_0 = 1.20$ fm. The values for (a) and (c) have been used previously by Ponomarev *et al.* [10] in the study of the DGDR in ^{136}Xe , while case (b) represents the choice of Boretzky *et al.* [9] [Fig. 2 corresponds to case (b)]. The cross sections for the GDR and the DGDR in ^{208}Pb incident on various nuclei are given in Table I where the three cases for R_{\min} are compared with the measured cross sections [9]. The intermediate value of R_{\min} [case (b)] reproduces the measured cross sections of the DGDR fairly well, but overestimates those of the GDR. On the other hand, the larger value [case (a)] reproduces the measured cross sections of GDR, while underestimating those of the DGDR by a factor of 2–3. In our calculation it seems impossible to simultaneously explain the measured GDR and DGDR cross sections with the same value of R_{\min} .

In the particle-vibration coupling calculation of the DGDR in ^{136}Xe by Ponomarev *et al.* [10], similar results for the cross section have been obtained, but the discrepancy between the measured cross section and their estimate is larger than that in our results. On the other hand, the simple folding model analysis of the DGDR in ^{208}Pb by Boretzky *et al.* [9] predicts only a 33% enhancement of the DGDR cross section while reproducing the GDR cross section. It

TABLE I. The energy-integrated cross section for Coulomb excitation of the GDR and DGDR in a ^{208}Pb projectile incident on U, Pb, Ho, and Sn targets at 640 MeV/A.

		(a)	(b)	(c)	exp
U	GDR	4.21	5.38	6.26	3.66
	DGDR	0.229	0.521	0.864	0.51
Pb	GDR	3.50	4.46	5.16	3.28
	DGDR	0.168	0.377	0.617	0.38
Ho	GDR	2.51	3.18	3.65	2.47
	DGDR	0.095	0.210	0.335	0.28
Sn	GDR	1.53	1.93	2.19	1.45
	DGDR	0.040	0.086	0.134	0.07

remains an open question whether this difference between results from the microscopic models and the folding model originates from the nuclear structure or from the treatment of the reaction mechanism.

In summary, we have carried out microscopic calculations for double-dipole excitations in ^{208}Pb using a realistic model space of $1p1h$ and $2p2h$ states. Since the number of $2p2h$ states in heavy nuclei is prohibitively large we have introduced the selection procedure [see Eq. (1)] as well as a truncation in the $2p2h$ energy. Although the width of DGDR may not be totally reliable because of this procedure, we believe that both the mean energy and the integrated strength are realistic.

The double-dipole strength is shown to be concentrated in an energy region twice that of the isovector giant dipole resonance, in good agreement with experiment, thus indicating that anharmonicity effects may be small. Based on the second-order perturbation theory the Coulomb cross section has been calculated. It depends sensitively on the minimum impact parameter, which appears in the semiclassical treatment of the cross section. We have estimated the cross section of the GDR and DGDR for three choices of the minimum impact parameter, available from the literature. None of these choices can explain the measured cross sections simultaneously and hence the discrepancy between measured cross sections and theoretical estimates, observed previously, remains.

We thank G. Baur and H. Emling for fruitful discussions. This work was supported in part by a grant from the National Science Foundation, No. NSF PHY94-21309.

[1] S. Mordechai *et al.*, Phys. Rev. Lett. **60**, 408 (1988); **61**, 531 (1988).
[2] J. Ritman *et al.*, Phys. Rev. Lett. **70**, 533 (1993); R. Schmidt *et al.*, *ibid.* **70**, 1767 (1993); T. Aumann *et al.*, Phys. Rev. C **47**, 1728 (1993).
[3] H. Emling, Prog. Part. Nucl. Phys. **33**, 729 (1994); Ph. Chomaz and N. Francaria, Phys. Rep. **252**, 275 (1995).
[4] S. Nishizaki and J. Wambach, Phys. Lett. B **349**, 7 (1995).

[5] S. Veyssiere *et al.*, Nucl. Phys. **A159**, 561 (1970).
[6] A. Winther and K. Alder, Nucl. Phys. **A319**, 518 (1979); K. Alder and A. Winther, *Coulomb Excitation* (Academic, New York, 1966).
[7] C. A. Bertulani and G. Baur, Phys. Rep. **163**, 299 (1988).
[8] S. Typel and G. Baur, Phys. Rev. C **50**, 2104 (1994).
[9] K. Boretzky *et al.*, Phys. Lett. B **384**, 30 (1996).
[10] V. Yu. Ponomarev *et al.*, Phys. Rev. Lett. **72**, 1168 (1994).